JOC The Journal of Organic Chemistry

Note

pubs.acs.org/joc

Strained and Unstrained Macrocycles Composed of Carbazole and Butadiyne Units: Electronic State and Optical Properties

Tomohito Ide,[†] Sho Sakamoto,[‡] Daisuke Takeuchi,[†] Kohtaro Osakada,*[,†] and Shigeru Machida[†,‡]

[†]Chemical Resources Laboratory, Tokyo Institute of Technology, 4259 Nagatsuta, Midori-ku, Yokohama 226-8503 (Mail Box R1-03), Japan

[‡]Department of Chemical Science and Engineering, Tokyo National College of Technology, 1220-2, Kunugida-machi, Hachioji, Tokyo 193-0997, Japan

Supporting Information

ABSTRACT: $Cu(OAc)_2$ catalyzes dehydrogenative condensation of 3,6-bis(2-ethynylphenyl)carbazole in the presence of O_2 to afford the cyclization product **1** and cyclodimer **2**. Compound **1** contains bent carbazole and butadiyne groups, while **2** has a less strained structure with Z shape around the two parallel butadiyne groups. Optical properties of the compounds are discussed based on the electronic states estimated from electrochemical measurement and density functional theory calculation.

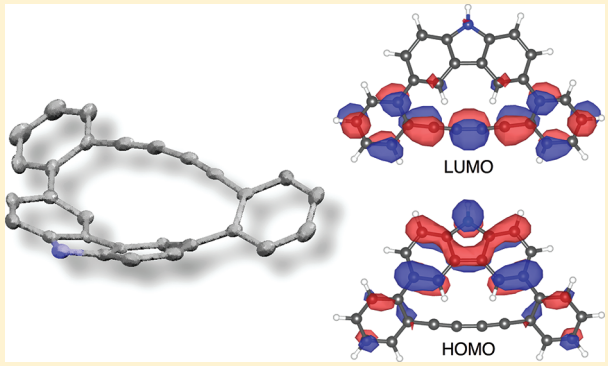

Strained macrocyclic molecules with bent π-conjugated systems, such as cyclophanes, show characteristic linear and nonlinear optical properties as well as redox behaviors.[1] Properties of [*n*]cycloparaphenylenes vary depending on their ring size;[2] smaller cycloparaphenylenes, for example, exhibit longer fluorescence wavelength and lower oxidation potential than the larger ones.[2a,d] Octadehydrodibenzo[12]annulene, which has strained butadiyne units, shows fluorescence maximum at 532 nm in spite of its small π-conjugated system.[3] Although many strained hydrocarbon macrocycles containing a bent π-conjugated system have been reported,[4] there are a limited number of those having heteroaromatic units.[5] Herein we report the synthesis, structure, and electronic state of macrocyclic molecules composed of carbazole and diphenylbutadiyne units. They are expected to exhibit characteristic properties derived from the strained ring system and the presence of a photo- and electrochemically active carbazole group.

Scheme 1 outlines the synthesis of carbazole−diphenylbutadiyne hybrid macrocycles **1** and **2**. 2-(Triisopropylsilylethynyl)-benzeneboronic acid **3** was obtained by Sonogashira coupling of 1-bromo-2-iodobenzene with (triisopropylsilyl)acetylene (99% yield) and boration (89% yield). Suzuki coupling reaction of **3** with 3,6-dibromocarbazole **4** formed **5** (91% yield), which was converted into **6** by removal of the TIPS groups with TBAF (84% yield). Addition of $Cu(OAc)_2$ catalyst to a dilute solution of **6** (pyridine/ether = 3:1, 10 mM) and stirring the solution for 40 h under air caused intra- and intermolecular coupling of the alkynyl groups to afford a mixture of cyclization product **1** and cyclic codimer **2**. These macrocyclic compounds were isolated in 38 and 10% yields, respectively, after purification using silica gel column chromatography.

X-ray analysis of **1** revealed its cyclic structure with ring strain (Figure 1a,b). The inner C−C≡C bond angles (169.8 and 169.9°) are deviated from those of strain-free linear diphenyl-1,3-butadiyne. The distortion is less significant than that of butadiyne units in octadehydrodibenzo[12]annulene (C−C≡C angle = 12.6−15.0°).[6] The carbazole unit is also distorted, and the angles between the five-membered ring and the six-membered rings are 13.2 and 14.4°. The ^{13}C NMR peaks of alkyne carbons of **1** are shifted to downfield (see Supporting Information). It can be ascribed to decrease of sp character and increase of sp^2 character due to the bent structure. DFT computation of a homodesmic reaction in Scheme 2[7] by accurate B2GP-PLYP-D3[8]/def2-TZVPP level of theory using BLYP-D3/def2-SVP level geometry computed by ORCA[9] indicated that the molecular strain energy (64.7 kJ mol^{-1}) was in the same range of octadehydrodibenzo[12]annulene (69.1 kJ mol^{-1}) calculated similarly.

Preliminary X-ray diffraction study of **2** revealed its molecular structure having two carbazole units whose NH groups are orientated to the opposite direction, as shown in Scheme 1.[10] The structure with two "Z"-shaped groups linked with two carbazole groups is confirmed by theoretical calculation (vide infra). Compound **2** showed sharp ^1H NMR signals at 60 °C (see Supporting Information), whereas some of the aromatic hydrogen signals are broadened at room temperature. The

Received: March 3, 2012
Published: April 23, 2012

Scheme 1. Synthesis of Carbazole–Diphenylbutadiyne Hybrid Macrocycles

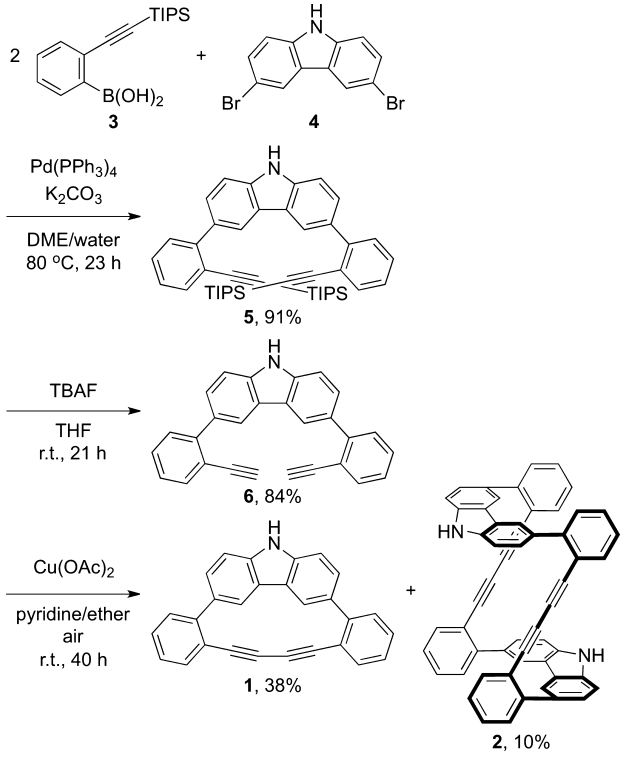

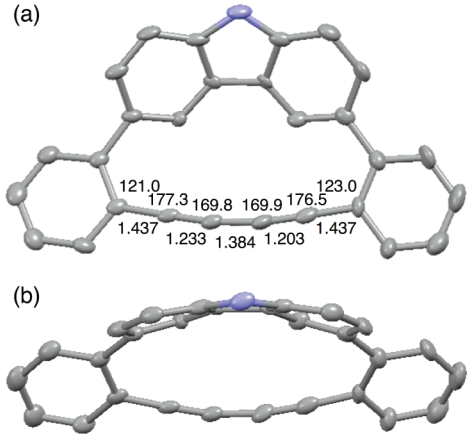

Figure 1. Thermal ellipsoid drawings of **1** with selected bond lengths (Å) on bottom and bond angles (°) on top.

Scheme 2. Homodesmic Reaction for Estimation of Strain Energy of 1

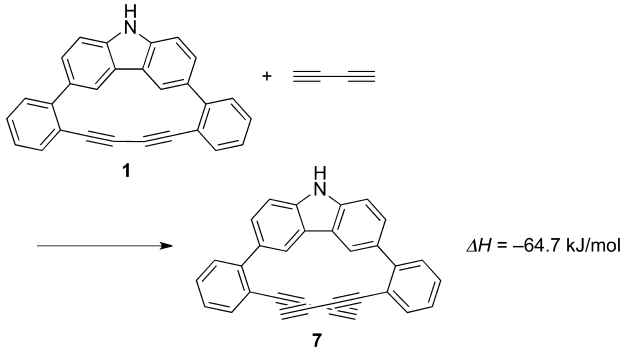

temperature-dependent change of the NMR spectrum can be assigned to fluxional behavior of the molecule such as synchronized rotation of the carbazole–phenyl single bonds.

UV–vis absorption and fluorescence spectra of **1** and **2** in $CHCl_3$ are shown in Figure 2. Weak absorption peak of **1** at

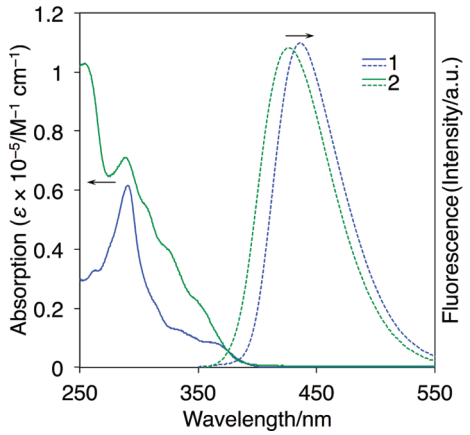

Figure 2. UV–vis absorption spectra (solid line) and fluorescence spectra (hashed line) of **1** and **2** in $CHCl_3$ (c = 0.01 mM for UV–vis and c = 0.001 mM for fluorescence spectra).

366 nm is assigned to charge-transfer (CT)-type absorption. Bathochromism of **1** was observed in THF due to CT nature of excitation (see Supporting Information). TD-DFT (BHLYP/def2-TZVP//BLYP-D3/def2-SVP) calculation suggested that the first transition of **1** (calculated to be 360 nm with oscillator strength f = 0.26) mainly consists of transition from HOMO delocalized on the carbazole unit to LUMO delocalized on the diphenylbutadiyne unit (Figure 3). The onset of absorption in

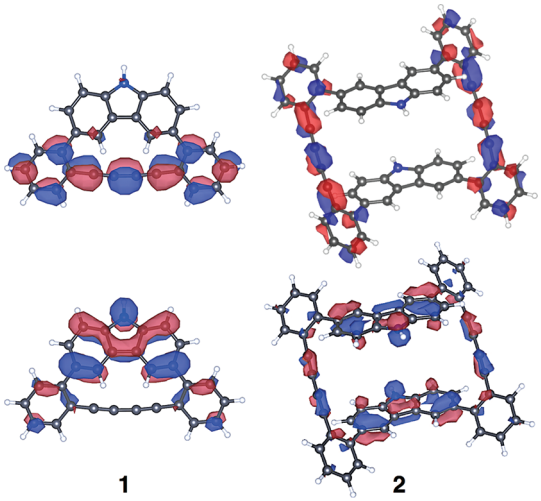

Figure 3. Frontier orbitals (B3LYP/def2-SVP//BLYP-D3/def2-SVP) of **1** and **2**. Plots (isosurface = 0.03) of LUMO (top) and HOMO (bottom).

the UV–vis spectra of **1** and **2** is observed at 390 and 382 nm, respectively. Since the wavelength corresponds to the energy gap of π–π^* transition, the energy gap of **1** is comparable to that of **2** regardless of the bent structure of **1**.

Table 1 summarizes HOMO, LUMO, and energy gaps of **1**, **2**, and **6**. Results of related compounds **1F** and **6F** having a fluorene group instead of the carbazole group of **1** and **6** are

dx.doi.org/10.1021/jo300441k | J. Org. Chem. 2012, 77, 4837–4841

Table 1. HOMO, LUMO, and Energy Gaps of Macrocycles 1, 2, Precursor 6, and Their Analogues 1F and 6F Calculated by B3LYP/def2-SVP//BLYP-D3/def2-SVP Level of theory

compound	HOMO/eV	LUMO/eV	energy gap/eV
1	−5.53	−1.92	3.61
2	−5.34	−1.71	3.63
6	−5.44	−1.15	4.29
1F[a]	−5.59	−2.05	3.54
6F[a]	−5.83	−1.27	4.56

[a]Chemical structures of **1F** and **6F** are shown below.

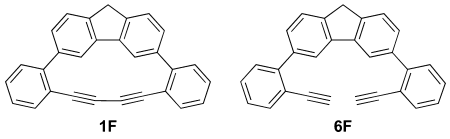

also included for comparison (B3LYP/def2-SVP//BLYP-D3/def2-SVP level). The HOMO level of **1** is slightly lower than that of **6** in spite of the strained structure. The relative HOMO levels are confirmed by electrochemical oxidation potential of the compounds, shown in Figure 4. The first oxidations of **1**

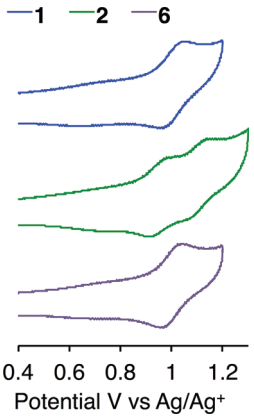

Figure 4. Cyclic voltammograms of **1**, **2**, and **6** (0.20 mM) in CH_2Cl_2 containing 0.10 M nBu$_4$N·PF$_6$.

(E_{pa} = 1.05 vs Ag/Ag$^+$) and **6** (E_{pa} = 1.04 V) are observed at the same potential in spite of the strained structure of **1**. Compound **2** shows double oxidation of two carbazole units (E_{pa} = 0.98 and 1.15 V), which is observed due to Coulomb repulsion by a carbazole cation of the mono-oxidized species. The above E_{pa} value indicated that the HOMO level of **2** is higher than that of **1**. It is contrasted with strained π-conjugated macrocycles such as [n]cycloparaphenylene,[2d] [n]-cyclothiophene,[4b] and six-porphyrin nanoring[4d] that undergo the first electrochemical oxidation at lower potentials than the corresponding linear molecules due to their higher HOMO level from ring strain.

The LUMO levels of **6**, **2**, and **1** are lowered in this order as shown in Table 1. Thus, the energy gap of **1** is comparable to that of **2** as expected from UV−vis spectra. Orbital energy levels of **1** and **6** are compared with **1F** and **6F** (Table 1) that have a fluorene group instead of the carbazole group of **1** and **6**. Although **1F** (and **6F**) is not prepared in this study, the optimized structure of **1F** is similar to that of **1**, and the angle between the five-membered ring and six-membered rings is 14.0°. The LUMO of **1F** is delocalized on the diphenylbutadiyne skeleton, and its level is roughly the same as that of **1**. The higher HOMO level of **1F** compared to that of **6F** is usual, although the macrocycle obtained in this study, **1** with the *N*-hetero-π-conjugated system, has a lower HOMO level than that of **6**. It is speculated that localization of the HOMO orbital on carbazole and electron-donating property of N atom are important factors for reversed order of HOMO level shifting.

The fluorescence maxima of **1** and **2** are observed at 436 nm (Φ_F = 0.038) and at 426 nm (Φ_F = 0.035), respectively. The red shift of **1** compared with **2** can be attributed to the ring strain. Photoexcitation of the carbazole ring is followed by electron transfer from the carbazole to the butadiyne group, consistent with the low Φ_F values because the fluorescence corresponds to the relaxation from the LUMO of **1**. Combination of the electron-poor butadiyne group and the electron-rich carbazole group resulted in the fluorescence properties via electron transfer from the photoexcitation state.

In summary, the macrocycle with bent carbazole **1** and its unstrained dimer **2** were newly synthesized, and their structures were revealed by X-ray crystallography. Electrochemical oxidation potential of the carbazole did not change in spite of the strained structure. DFT calculation suggested that the HOMO level of **1** is slightly lower than that of **2**. The strained *N*-hetero-π-conjugated system of **1** shows a different energy level shift on the frontier orbital from the hydrocarbon derivative **1F**. The levels and delocalization of the orbitals affected the optical properties of the strained molecule **1**.

EXPERIMENTAL SECTION

Synthesis. *1-Bromo-2-(triisopropylsilylethynyl)benzene.*[11] $PdCl_2(PPh_3)_2$ (35.1 mg, 0.050 mmol), CuI (14.0 mg, 0.074 mmol), Et_3N (80 mL), 1-bromo-2-iodobenzene (0.63 mL, 5.00 mmol), and triisopropylsilylacetylene (1.3 mL, 5.84 mmol) were placed in a Schlenk tube under argon. The mixture was stirred at room temperature for 12 h. The reaction mixture was evaporated to dryness. The residual oil was dissolved in hexane and through a short plug of silica gel. The solvent was removed, and the resulting oil was dried with heating under vacuum to give 1-bromo-2-(triisopropylsilylethynyl)benzene as colorless oil (1.68 g, 99%): ^{1}H NMR (500 MHz, $CDCl_3$) δ 7.59 (d, J = 8 Hz, 1H), 7.53 (dd, J = 8, 2 Hz, 1H), 7.26 (ddd, J = 8, 8, 1 Hz, 1H), 7.17 (ddd, J = 8, 8, 1 Hz, 1H), 1.18 (m, 21 H); ^{13}C NMR (125 MHz, $CDCl_3$) δ 133.8, 132.3, 129.3, 126.8, 125.7, 125.6, 104.7, 96.2, 18.7, 11.3.

*2-(Triisopropylsilylethynyl)benzeneboronic acid (**3**).* To a solution of 1-bromo-2-(triisopropylsilylethynyl)benzene (0.846 g, 2.5 mmol) in THF (25 mL) at −84 °C was added 2.6 M nBuLi in hexane (1.2 mL, 3.0 mmol). After 30 min, trimethyl borate (0.56 mL, 5.0 mmol) was added to the cold solution at the temperature. The reaction mixture was allowed to warm slowly to room temperature and was stirred for additional 12 h. The reaction mixture was quenched with 2 N HCl (20 mL). After the mixture was stirred for 1 h at room temperature, the reaction mixture was washed with water (×2) and brine and then extracted with hexane. The organic phases were dried over Na_2SO_4, and the solvent was removed under vacuum. Silica gel column chromatography (hexane/ethyl acetate 10:1) of the residue gave 2-(triisopropylsilylethynyl)benzeneboronic acid as a white solid (0.677 g, 89%): ^{1}H NMR (500 MHz, $CDCl_3$) δ 7.99 (d, J = 7 Hz, 1H), 7.54 (d, J = 7 Hz, 1H), 7.42 (tt, J = 7, 1 Hz, 1H), 7.39 (tt, J = 7, 1 Hz, 1H), 5.94 (s, 2H), 1.16 (m, 21 H); ^{13}C NMR (125 MHz, $CDCl_3$) δ 135.5, 133.1, 130.7, 128.4, 126.9, 108.4, 95.8, 18.6, 11.3; HRMS (ESI-TOF-MS) calcd for $C_{34}H_{52}B_2O_3Si_2$ + Na 609.3546, found m/z = 609.3549 [2M − H_2O + Na^+], dehydrated dimer was observed.

*3,6-Bis(2-(triisopropylsilylethynyl)phenyl)carbazole (**5**).* A mixture of 2-(triisopropylsilylethynyl)benzeneboronic acid **4** (321 mg, 1.1 mmol), $Pd(PPh_3)_4$ (60.8 mg, 0.053 mmol), K_2CO_3 (368 mg, 2.7 mmol), 3,6-dibromocarbazole **3** (156 mg, 0.48 mmol), degassed water (50 mL), and dimethoxyethane (50 mL) was stirred at 80 °C in argon for 23 h. The reaction mixture was washed with water and brine and

dx.doi.org/10.1021/jo300441k | J. Org. Chem. 2012, 77, 4837−4841

then extracted with ethyl acetate. The solvent was evaporated under vacuum. The residue was purified by silica gel column chromatography (hexane/ethyl acetate 5:1) to give 3,6-bis(2-(triisopropylsilylethynyl)-phenyl)carbazole as a pale yellow oil (298 mg, 91%): ^{1}H NMR (500 MHz, $CDCl_3$) δ 8.42 (d, J = 1 Hz, 2H), 8.11 (s, 1H), 7.72 (dd, J = 8, 1 Hz, 2H), 7.64 (dd, J = 7, 1 Hz, 2H), 7.48 (dd, J = 8, 1 Hz, 2H), 7.43 (d, J = 8 Hz, 2H), 7.39 (ddd, J = 8, 1 Hz, 2H), 7.28 (ddd, J = 7, 1 Hz, 2H), 0.94 (m, 21 H); ^{13}C NMR (125 MHz, $CDCl_3$) δ 145.3, 139.5, 134.1, 132.4, 130.0, 128.7, 127.9, 126.5, 123.7, 122.4, 121.5, 110.0, 107.0, 93.7, 18.7, 17.9, 12.5, 11.5; HRMS (ESI-TOF-MS) calcd for $C_{46}H_{57}NSi_2$ + Na 702.3922, found m/z = 702.3916 [M + Na^+].

*3,6-Bis(2-ethynylphenyl)carbazole (**6**).* To a solution of 3,6-bis(2-(triisopropylsilylethynyl)phenyl)carbazole **5** (260 mg, 0.38 mmol) in THF (8 mL) was added 1 M TBAF in THF (0.36 mL, 0.36 mmol) at room temperature. After stirred for 21 h at room temperature, the reaction mixture was washed with water (×2) and brine and then extracted with ethyl acetate. The organic phase was dried over Na_2SO_4, and the solvent was evaporated to dryness. Silica gel column chromatography (hexane/ethyl acetate 1:4) of the residue gave 3,6-bis(2-ethynylphenyl)carbazole as a pale yellow solid (118 mg, 84%): ^{1}H NMR (500 MHz, $CDCl_3$) δ 8.32 (d, J = 1 Hz, 2H), 8.15 (s, 1H), 7.68 (dd, J = 9, 2 Hz, 2H), 7.66 (d, J = 7 Hz, 2H), 7.51−7.43 (m, 4H), 7.44 (ddd, J = 7, 1 Hz, 2H), 7.31 (ddd, J = 7, 1 Hz, 2H); ^{13}C NMR (125 MHz, $CDCl_3$) δ 145.2, 139.4, 133.9, 131.9, 130.0, 129.0, 127.5, 126.5, 123.4, 121.2, 120.6, 110.1, 83.6, 79.9; HRMS (ESI-TOF-MS) calcd for $C_{28}H_{17}N$ + Na 390.1253, found m/z = 390.1251 [M + Na^+].

*Macrocycles **1** and **2**.* 3,6-Bis(2-ethynylphenyl)carbazole **6** (97.0 mg, 0.27 mmol) and $Cu(OAc)_2{\cdot}2H_2O$ (299 mg, 1.6 mmol) were dissolved in pyridine (20 mL) and diethyl ether (7 mL). The mixture was stirred at room temperature under air for 44 h. The reaction mixture was washed with saturated aqueous NH_4Cl (×2) and then extracted with ethyl acetate. The organic phase was dried over Na_2SO_4, and the solvent was removed under vacuum. The residue was subjected to silica gel chromatography (hexane/ethyl acetate 3:1 then 2:1) to afford **1** and **2** from different fractions. Each product was washed with a small amount of acetonitrile to give **1** as a yellow solid (35.4 mg, 38%) and **2** as an ivory solid (10.1 mg, 10%). **1**: ^{1}H NMR (500 MHz, THF-d_8) δ 10.43 (s, 1H), 8.84 (d, J = 1 Hz, 2H), 7.86 (d, J = 8 Hz, 2H), 7.54 (d, J = 8 Hz, 2H), 7.46 (ddd, J = 7, 1 Hz, 2H), 7.40 (d, J = 8 Hz), 7.38 (dd, J = 8, 2 Hz, 2H), 7.25 (ddd, J = 7, 1 Hz, 2H); ^{13}C NMR (125 MHz, $CDCl_3$) δ 146.9, 142.9, 133.7, 130.3, 130.3, 128.7, 127.0, 126.9, 125.1, 124.9, 122.0, 112.0, 88.2, 80.5; HRMS (ESI-TOF-MS) calcd for $C_{28}H_{15}N$ + Na 388.1097, found m/z = 388.1108 [M + Na^+]. **2**: ^{1}H NMR (500 MHz, THF-d_8, 60 °C) δ 10.0 (s, 2H), 7.85 (s, 4H), 7.57 (d, J = 8 Hz, 4H), 7.48 (d, J = 8 Hz, 4H), 7.40 (m, 12H), 7.24 (ddd, J = 7, 2 Hz, 4H); ^{13}C NMR (125 MHz, $CDCl_3$) δ 147.9, 141.2, 134.6, 132.4, 130.8, 129.7, 127.1, 124.6, 122.4, 120.9, 110.7, 82.1, 76.9; HRMS (ESI-TOF-MS) calcd for $C_{56}H_{30}N_2$ + Na 753.2301, found m/z = 753.2294 [M + Na^+]. Melting point of **1** was not determined by DSC measurement probably because of thermal decomposition.

Computational Methods. Geometry optimization was performed by BLYP-D3/def2-SVP level of theory with the resolution of the identity (RI) approximation. Stationary points were characterized by Hessian calculation. Single point energies were obtained by B2GP-PLYP-D3/def2-TZVPP together with RIJCOSX and RI approximation. Kohn−Sham orbitals were calculated by B3LYP/def2-SVP level of theory. TD-DFT calculations within the Tamm−Dancoff approximation (TD-DFT/TDA) were carried out by BHLYP/def2-TZVP level of theory in combination with RIJONX approximation. All calculations were performed by ORCA 2.8.0.2. The plots (isosurface = 0.03) of the frontier orbitals were drawn by VESTA 3.[12]

■ ASSOCIATED CONTENT

Supporting Information

NMR spectra, crystallographic parameters, and computational detail. This material is available free of charge via the Internet at http://pubs.acs.org.

■ AUTHOR INFORMATION

Corresponding Author

*E-mail: kosakada@res.titech.ac.jp.

Notes

The authors declare no competing financial interest.

■ ACKNOWLEDGMENTS

This work was supported by a Grant-in-Aid for Scientific Research on Innovation Areas, "Coordination Programming" (22108509) from the Ministry of Education, Culture, Sports, Science, and Technology, Japan. T.I. acknowledges a Research Fellowship for Young Scientists from the Japan Society for the Promotion of Science.

■ REFERENCES

(1) (a) Cram, D. J.; Cram, J. M. *Acc. Chem. Res.* **1971**, *4*, 204−213. (b) Kawase, T.; Kurata, H. *Chem. Rev.* **2006**, *106*, 5250−5273. (c) Jasti, R.; Bertozzi, C. R. *Chem. Phys. Lett.* **2010**, *494*, 1−7. (d) Iyoda, M.; Yamakawa, J.; Rahman, M. J. *Angew. Chem., Int. Ed.* **2011**, *50*, 10522−10553.

(2) (a) Jasti, R.; Bhattacharjee, J.; Neaton, J. B.; Bertozzi, C. R. *J. Am. Chem. Soc.* **2008**, *130*, 17646−17647. (b) Yamago, S.; Watanabe, Y.; Iwamoto, T. *Angew. Chem., Int. Ed.* **2010**, *49*, 757−759. (c) Omachi, H.; Matsuura, S.; Segawa, Y.; Itami, K. *Angew. Chem., Int. Ed.* **2010**, *49*, 10202−10205. (d) Iwamoto, T.; Watanabe, Y.; Sakamoto, Y.; Suzuki, T.; Yamago, S. *J. Am. Chem. Soc.* **2011**, *133*, 8354−8361. (e) Sisto, T. J.; Golder, M. R.; Hirst, E. S.; Jasti, R. *J. Am. Chem. Soc.* **2011**, *133*, 15800−15802.

(3) Setaka, W.; Kanai, S.; Kabuto, C.; Kira, M. *Chem. Lett.* **2006**, *35*, 1364−1365.

(4) (a) Brown, C. J.; Farthing, A. C. *Nature* **1949**, *164*, 915−916. (b) Kawase, T.; Ueda, N.; Darabi, H. R.; Oda, M. *Angew. Chem., Int. Ed. Engl.* **1996**, *35*, 1556−1558. (c) Kawase, T.; Darabi, H. R.; Oda, M. *Angew. Chem., Int. Ed. Engl.* **1996**, *35*, 2664−2666. (d) Collins, S. K.; Yap, G. P. A.; Fallis, A. G. *Angew. Chem., Int. Ed.* **2000**, *39*, 385−388. (e) Seiders, T. J.; Baldridge, K. K.; Siegel, J. S. *Tetrahedron* **2001**, *57*, 3737−3742. (f) Hisaki, I.; Eda, T.; Sonoda, M.; Tobe, Y. *Chem. Lett.* **2004**, *33*, 620−621. (g) Merner, B. L.; Dawe, L. N.; Bodwell, G. J. *Angew. Chem., Int. Ed.* **2009**, *48*, 5487−5491. (h) Standera, M.; Häfliger, R.; Gershoni-Poranne, R.; Stanger, A.; Jeschke, G.; van Beek, J. D.; Bertschi, L.; Schlüter, A. D. *Chem.—Eur. J.* **2011**, *17*, 12163−12174.

(5) (a) Nakao, K.; Nishimura, M.; Tamachi, T.; Kuwatani, Y.; Miyasaka, H.; Nishinaga, T.; Iyoda, M. *J. Am. Chem. Soc.* **2006**, *128*, 16740−16747. (b) O'Connor, M. J.; Yelle, R. B.; Zakharov, L. N.; Haley, M. M. *J. Org. Chem.* **2008**, *73*, 4424−4432. (c) Zhang, F.; Götz, G.; Winkler, H. D. F.; Schalley, C. A.; Bäuerle, P. *Angew. Chem., Int. Ed.* **2009**, *48*, 6632−6635. (d) O'Sullivan, M. C.; Sprafke, J. K.; Kondratuk, D. V.; Rinfray, C.; Claridge, T. D. W.; Saywell, A.; Blunt, M. O.; O'Shea, J. N.; Beton, P. H.; Malfois, M.; Anderson, H. L. *Nature* **2011**, *469*, 72−75. (e) Sprafke, J. K.; Kondratuk, D. V.; Wykes, M.; Thompson, A. L.; Hoffmann, M.; Drevinskas, R.; Chen, W.-H.; Yong, C. K.; Kärnbratt, J.; Bullock, J. E.; Malfois, M.; Wasielewski, M. R.; Albinsson, B.; Herz, L. M.; Zigmantas, D.; Beljonne, D.; Anderson, H. L. *J. Am. Chem. Soc.* **2011**, *133*, 17262−17273.

(6) Zhou, Q.; Carroll, P. J.; Swager, T. M. *J. Org. Chem.* **1994**, *59*, 1294−1301.

(7) (a) George, P.; Trachtman, M.; Bock, C. W.; Brett, A. M. *Tetrahedron* **1976**, *32*, 317−323. (b) George, P.; Trachtman, M.; Brett, A. M.; Bock, C. W. *J. Chem. Soc., Perkin Trans. 2* **1977**, 1036−1047.

(8) (a) Karton, A.; Tarnopolsky, A.; Lamère, J.-F.; Schatz, G. C.; Martin, J. M. L. *J. Phys. Chem. A* **2008**, *112*, 12868−12886. (b) Goerigk, L.; Grimme, S. *J. Chem. Theory Comput.* **2011**, *7*, 291−309.

(9) Neese, F. *ORCA*, version 2.8.0.2; University of Bonn: Bonn, Germany, 2011. http://www.thch.uni-bonn.de/tc/orca.

(10) Detailed bond parameters of the molecule of **2** were not determined by X-ray crystallography. Crystallographic parameters: a = 13.70(2) Å, b = 15.19(2) Å, c = 18.36(2) Å, α = 78.17(4)°, β = 87.72(5)°, γ = 85.76(3)°. Two acetonitrile molecules are contained in the cavity of the macrocycle in the crystals.
(11) Felber, B.; Diederich, F. *Helv. Chim. Acta* **2005**, *88*, 120−153.
(12) Momma, K.; Izumi, F. *J. Appl. Crystallogr.* **2008**, *41*, 653−658.

dx.doi.org/10.1021/jo300441k | *J. Org. Chem.* 2012, 77, 4837−4841